Supporting Information

Investigation of Ultraviolet Optical Properties of Semiconducting-enriched and Metal-enriched Single-Walled Cabon Nanotube Network Using Spectroscopic Ellipsometry

Young Ran Park[a], Woo-Jae Kim[b], Min Jae Ko[c], Nam-Ki Min[d], and Cheol Jin Lee*[a]

[a] School of Electrical Engineering, Korea University, Seoul 136-713, Republic of Korea.

[b] Department of Chemical and Environmental Engineering, Gachon University, Sungnam, Gyeonggi-do 461-701, Republic of Korea

[c] Photo-Electronic Hybrid Research Center, Korea Institute of Science and Technology, Hwarangno 14-gil 5, Seongbuk-gu, Seoul 136-791, Republic of Korea

[d] Department of Control and Instrumentation Engineering, Korea University, Chungnam 339-700, Republic of Korea

*Corresponding author. E-mail : cjlee@korea.ac.kr

3. Results

Figure 3 shows the in-plane ($\psi = 90^o$) XRD patterns of the θ-2ω scans obtained for HRGIXD. In the in-plane ($\psi = 90^o$) θ-2ω scans, the reciprocal space is probed in the *z* direction (q_z, where **q** is the scattering vector and *z* is perpendicular to the sample surface), and therefore planes parallel to the surface can be investigated with these measurements. The transformation between the measured angles and reciprocal space was performed by using the following expression, where λ is the wavelength and 2θ is the diffraction angle:

$$q_z = \frac{2\pi}{d} = \frac{4\pi}{\lambda}\sin\left(\frac{2\theta}{2}\right) \qquad (1)$$

During the SWCNT formation process van der waals forces lead to the creation of bundles of SWCNT's in which the individual nanotubes are arranged within a hexagonal lattice. Generally, the peaks in a SWCNT's diffraction profile can be divided into two parts. The low-q part of the diffraction pattern (below $2Å^{-1}$) is only sensitive to the crystalline order in the bundle, thus corresponding to SWCNT bundle diffraction. The high-q range (above 2 $Å^{-1}$) is sensitive to the internal structure of individual tubes, whereby the peaks near 2.9 and 5 $Å^{-1}$ originate from the (100) and (110) graphite in-plane reflections, respectively.

The diffraction pattern of SWCNT bundles can be described as the association of the carbon nanotube form factor, and the Bragg reflections from the two-dimensional (2D) hexagonal lattice of the nanotubes in bundles. The most intense peak in the calculated diffraction pattern is the (10) reflection located at ~0.4 $Å^{-1}$ and the higher q values the (11), (20), (21), and (22)+(31) reflection can be observed at 0.75, 0.9, 1.1, and 1.5 Å, respectively. The absence of the (10) peak (0.4 $Å^{-1}$) is related to the adsorption/intercalation of air or other molecules into the SWCNT during or after deposition film.[1] Desorption/de-intercalation occurred upon heating. It previously been established that oxygen species adsorbed on the surface of SWCNT can act as hole dopants in SWCNT films.[2]

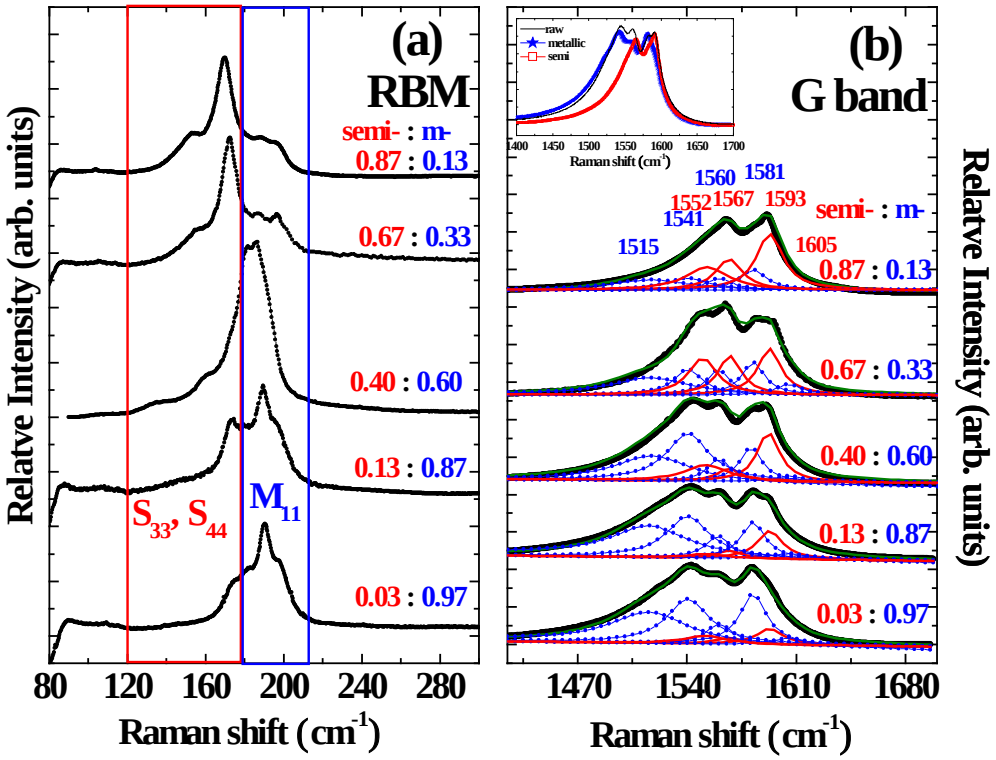

Figure S1. The micro Raman spectra of the semi-/m- separated SWCNTs at an excitation energy of 1.96 eV (633 nm). (a) Radial breathing modes (RBMs) and (b) G-band; Red and blue colors are semiconducting and metallic SWCNTs, respectively.

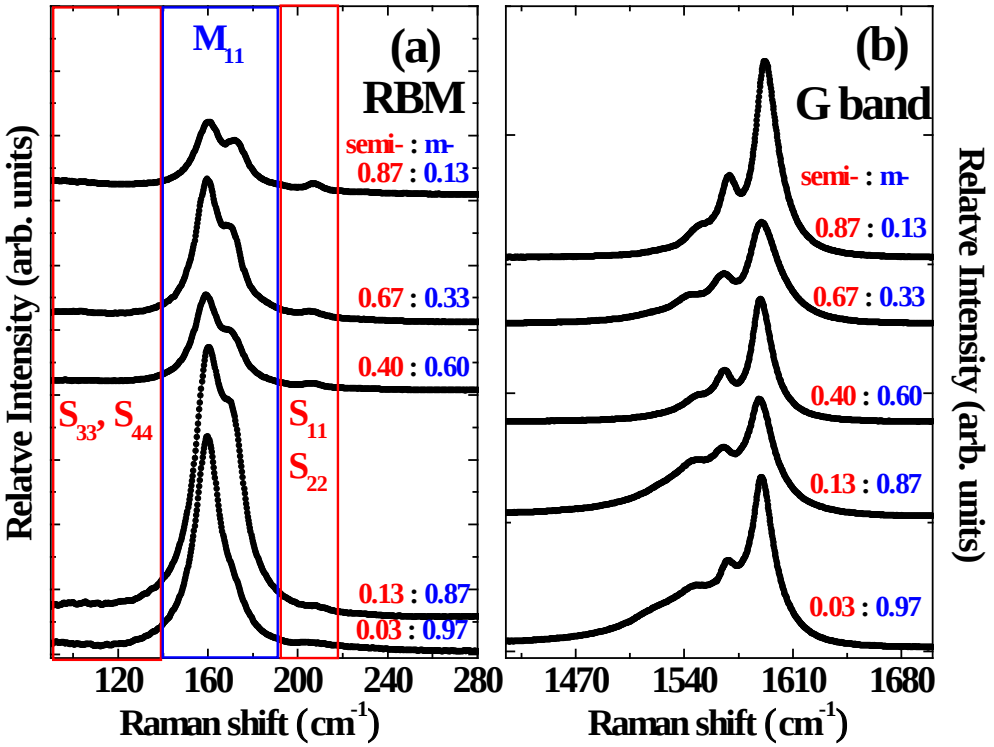

Figure S2. The micro Raman spectra of the semi-/m- separated SWCNTs at an excitation energy of 1.58 eV (785 nm). (a) Radial breathing modes (RBMs) and (b) G-band; Red and blue colors are semiconducting and metallic SWCNTs, respectively.

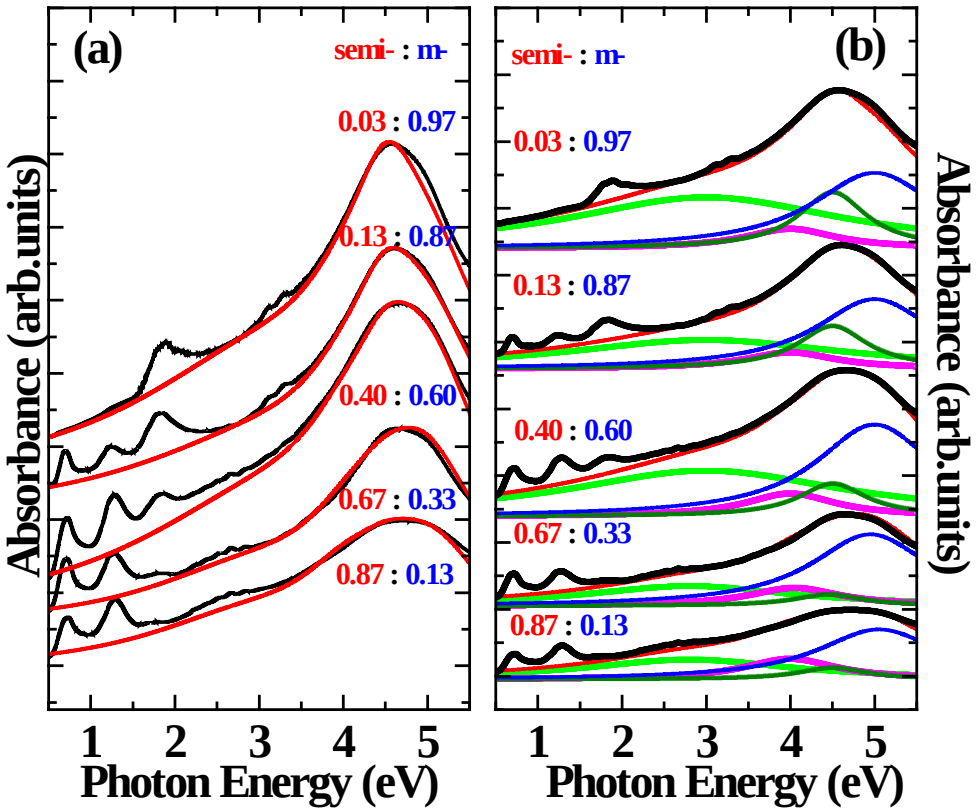

Figure S3. (a) Original optical absorbance spectra (black lines) and their corresponding baseline (red lines), (b) Fitting of measured absorbance spectra presented in Fig. 1 by four Lorentzian curves ; The red, blue, green, pink, and yellowish-green lines are the summation of four Lorentzian, 5.0 eV, 4.5 eV, 4.0 eV, and 2.8 eV fitting curves, respectively. Their widths were fixed at 4.0, 1.3, 0.98, and 1.72 eV, respectively.

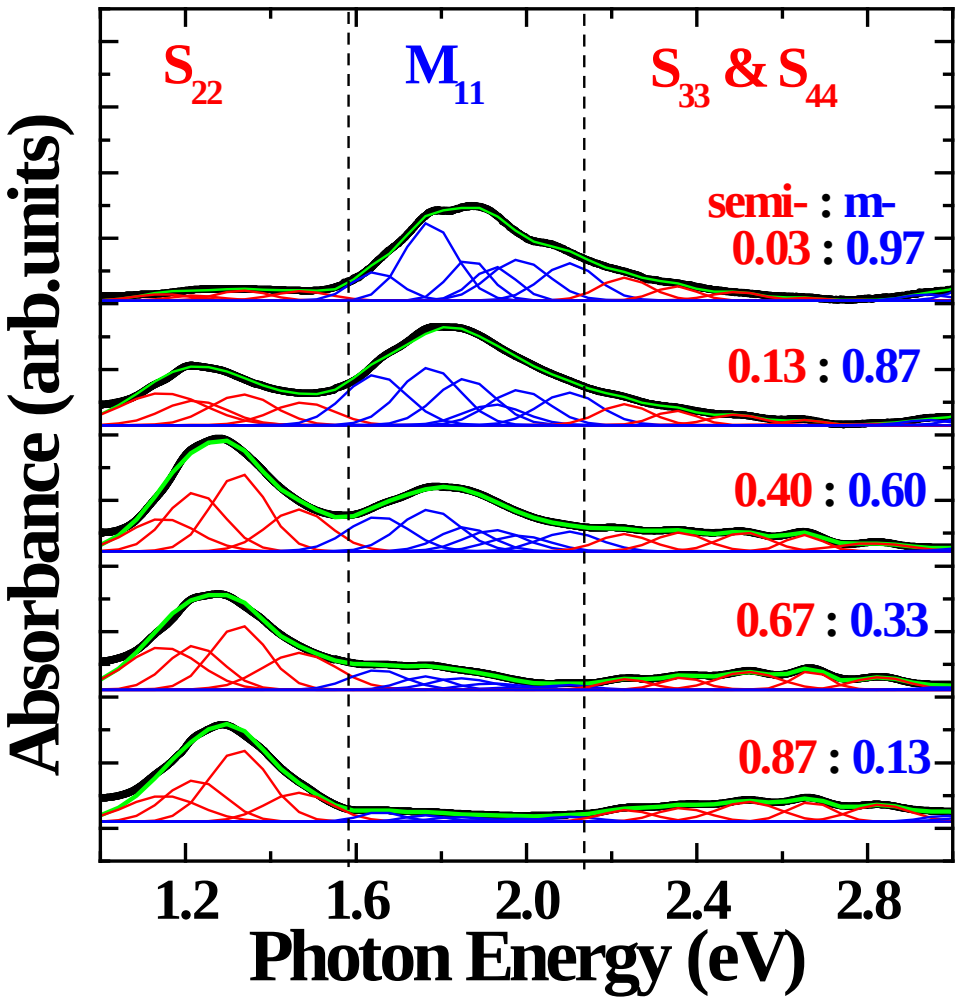

Figure S4. The UV-vis-NIR absorbance spectra of SWCNTs films after baseline correction (the black lines) with Gaussian fitting (the red, blue, and yellowish-green lines are semiconducting SWCNTs, metallic SWCNTs, and summation of the total fitted curves, respectively).

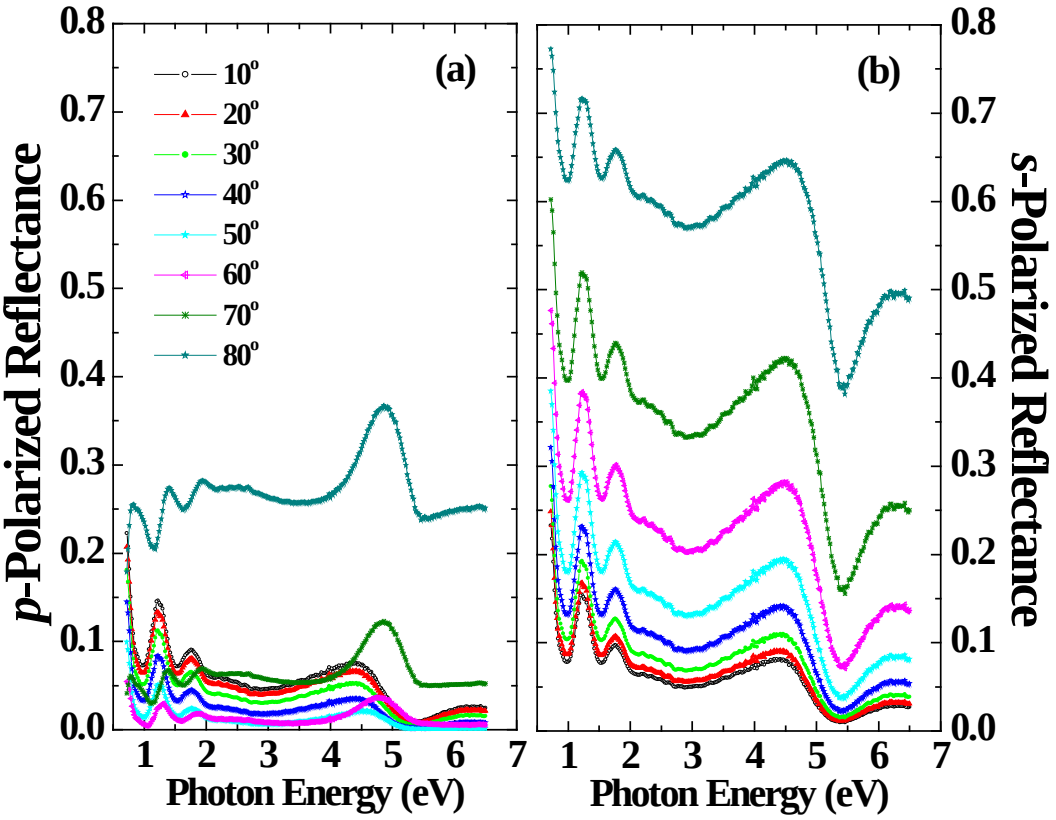

Figure S5. Angle-dependent reflectance spectra for a raw-SWCNT film on corning glass. The modeled data points for (a) *p*- and (b) *s*- polarized reflection spectra calculated using (VUV-VASE) from Ψ and Δ.

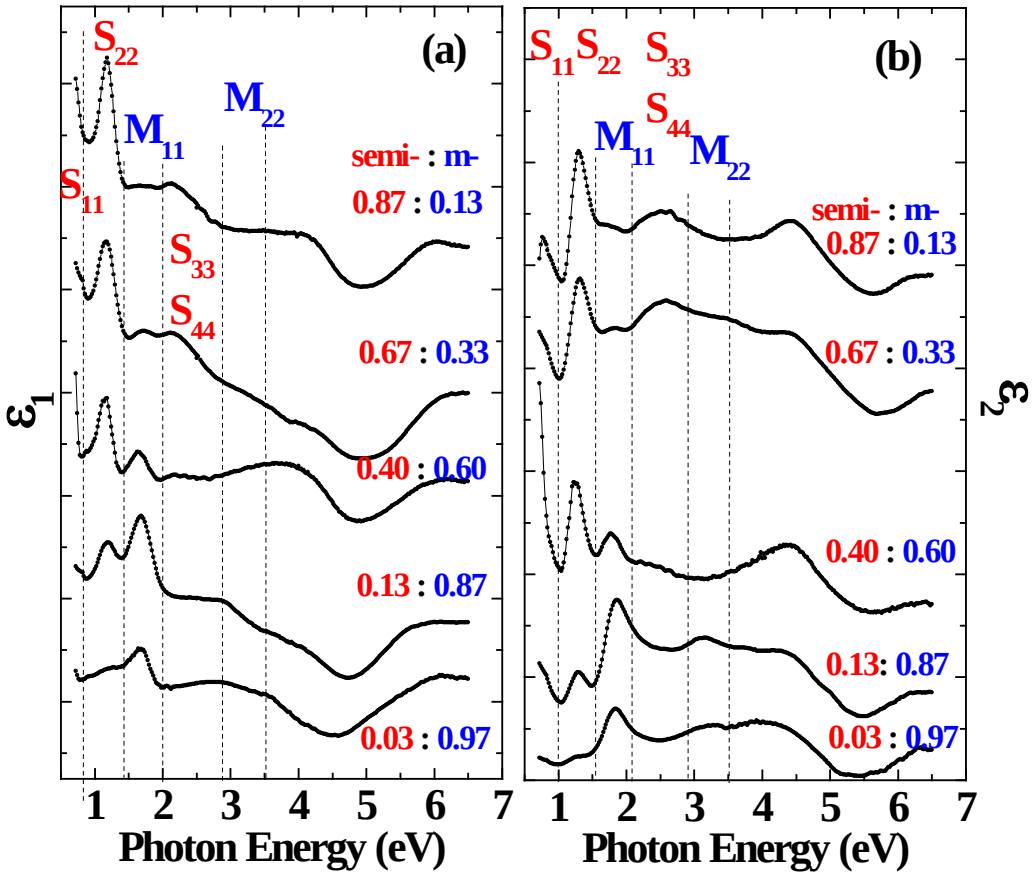

Figure S6. Real (a) and imaginary (b) parts of complex dielectric function of raw- SWCNTs compared with those of semiconducting-enriched and metallic-enriched SWCNTs.

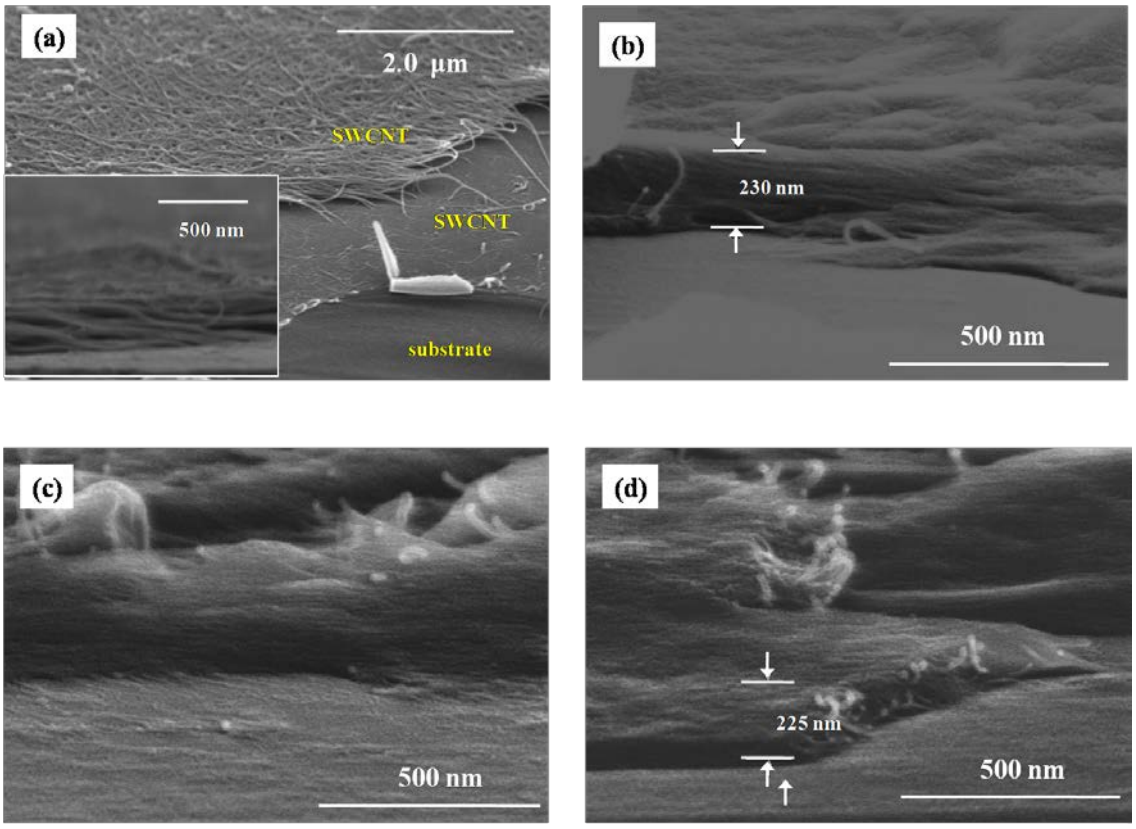

Figure S7. FESEM images of bundled and unbundled SWCNT film without and with using the ultracentrifugation process, respectively. (a) bundled raw-SWCNT film(0.4(semi)/0.6(m)), (b) unbundled raw-SWCNT film(0.4(semi)/0.6(m)) (c) unbundled semi- enriched SWCNT film (0.87(semi)/0.13(m)), and (d) unbundled m- enriched SWCNT film(0.03(semi)/0.97(m)).

Reference

[1] X. Liu, T. Pichler, M. Knupfer, J. Fink, *Phys. Rev. B* **2003**, 67, 125403.

[2] J. L. Blackburn, T. M. Barnes, M. C. Beard, Y.-H.Kim, R. C. Tenent, T. J. McDonald, B. To, T. J. Coutts, M. J. Heben, *ACS Nano* **2008**, 2, 1266-1274.